Published in final edited form as:
Cell. 2011 June 24; 145(7): 1102–1115. doi:10.1016/j.cell.2011.06.007.

Golgi Export of the Kir2.1 Channel is Driven by a Trafficking Signal Located within Tertiary Structure

Donghui Ma[†], **Tarvinder Kaur Taneja**[†], **Brian M. Hagen**, **Bo-Young Kim**, **Bernardo Ortega**, **W. Jonathan Lederer**, and **Paul A. Welling**[*]
Department of Physiology, University of Maryland School of Medicine Baltimore, MD 21201

Abstract

Mechanisms responsible for sorting newly synthesized proteins for traffic to the cell surface from the Golgi are poorly understood. Here we show that the potassium channel Kir2.1, mutations in which are associated with Andersen-Tawil Syndrome, is selected as cargo into Golgi export carriers in an unusual signal-dependent manner. Unlike conventional trafficking signals, which are typically comprised of short linear peptide sequences, Golgi exit of Kir2.1 is dictated by residues embedded within the confluence of two separate domains. This signal patch forms a recognition site for interaction with the AP1 adaptor complex, thereby marking Kir2.1 for incorporation into clathrin-coated vesicles at the trans-Golgi. The identification of a trafficking signal in the tertiary structure of Kir2.1 reveals a quality control step that couples protein conformation to Golgi export and provides molecular insight into how mutations in Kir2.1 arrest the channels at the Golgi.

INTRODUCTION

The Golgi apparatus is well appreciated to act as the central biosynthetic sorting station, responsible for properly targeting newly synthesized membrane proteins to their appropriate subcellular destinations (De Matteis and Luini, 2008). Endosomal sorting processes provide a framework for understanding the underlying molecular mechanisms. It is well established that endosome and lysosome-destined proteins are recognized at the Golgi as cargo for inclusion into clathrin-coated vesicles by short, linear tyrosine-containing or di-hydrophobic signals, which serve as recognition sites for interaction with clathrin adaptor complexes and GGA proteins (Bonifacino and Traub, 2003). Although much less is known about how newly synthesized plasma membrane proteins are sorted to the cell surface, an emerging body of evidence indicates that select plasmalemma proteins may also leave the Golgi by signal-dependent processes, rather than by default trafficking pathways as once believed (Rodriguez-Boulan and Musch, 2005). Subsets membrane proteins in polarized epithelial cells, for example, are sorted at the Golgi for traffic to the basolateral membrane in a clathrin-dependent manner (Deborde et al., 2008) by short linear peptide sequences(Campo et al., 2005). Although these signals share remarkable similarity with endosomal sorting signals, the clathrin-associated sorting proteins that interact with them at the Golgi remain to be discovered. Other cell surface proteins (see below) rely on completely unrelated structures for Golgi export and the sorting machineries that decode these putative signals

[*]Address correspondence to: Paul A. Welling, pwelling@umaryland.edu.
[†]These authors contributed equally and should be both considered as first authors

also remain unknown. Different coat proteins (Wang et al., 2006), Golgi tethers (Lock et al., 2005) and scaffolding molecules (Godi et al., 2004) have been implicated in Golgi-to-cell-surface traffic, but these are considered to play important roles in carrier vesicle formation rather than in cargo recognition.

Signal-dependent Golgi export processes have been implicated in controlling the surface density of inwardly rectifying K^+(Kir) channels (Nichols and Lopatin, 1997). In recent years, it has become evident that different trafficking processes regulate Kir channels to control neuronal excitability, action potential cessation, hormone secretion, heart rate and salt balance. Several Kir channels have been postulated to leave the Golgi in a signal-dependent manner (Stockklausner and Klocker, 2003; Yoo et al., 2005). In the Kir2.1 channel (Kubo et al., 1993), a short cluster of highly-conserved basic amino acids in the cytoplasmic N-terminus is required for Golgi-exit (Stockklausner and Klocker, 2003). A nearly identical structure in the kidney potassium channel, Kir1.1 (ROMK), is necessary for forward trafficking in the secretory pathway (Yoo et al., 2005), consistent with a shared signal-dependent Golgi export process. Nevertheless, the sequences exhibit no resemblance to known trafficking signals, and it is completely unknown how they might control Golgi exit.

In the present study, a human Kir2.1 channel disease, Andersen-Tawil syndrome (ATS1) (Plaster et al., 2001), provided a new insight into the Golgi mechanism. The Kir2.1 channel (Kubo et al., 1993), is responsible for controlling membrane excitability in many cell types. Because it is especially important in ventricular cardiomyocytes (Zaritsky et al., 2001) and skeletal muscle (Fischer-Lougheed et al., 2001), loss of Kir2.1 function in ATS1 is manifested as a disorder of ventricular arrhythmias, periodic paralysis, and skeletomuscular dysplasia (Andersen et al., 1971; Sansone et al., 1997). Of the many ATS1 mutations, we found one of them in the cytoplasmic C-terminus of Kir2.1 surprisingly blocks Golgi export. Our investigation into the underlying pathologic mechanism revealed that Golgi exit of Kir 2.1 is dictated by an unusual signal. Unlike conventional short, linear trafficking signals, the Golgi export signal in Kir2.1 is formed by a patch of residues located within the confluence of cytoplasmic N-and C-terminal domains. This signal patch creates an interaction site for the AP1 adaptin complex, allowing properly folded Kir2.1 channels to be incorporated into clathrin-coated vesicles at the trans-Golgi for export to the cell surface.

RESULTS

Kir 2.1 Channels, Bearing an ATS1 Mutation, Accumulate in the Golgi

Exploration of the Golgi-export mechanism in Kir2.1 was guided by mapping the location of an ATS1 mutation, Δ314-15 (Plaster et al., 2001), in the atomic resolution structure (Pegan et al., 2005). Remarkably, the involved C-terminal residues, SY_{315}, juxtapose the N-terminal Golgi trafficking determinant at a domain interface (Fig.1). The mutation has been reported to block surface expression (Bendahhou et al., 2003) but the mechanism is not known. Since our studies revealed the mutation does not impair subunit assembly, or cause misfolding or ER-retention (Fig. S1), we wondered if it might, instead, disrupt Golgi-trafficking and provide a model for understanding the export signal. In fact, Kir2.1Δ314-15 channels exhibit an unusual mistrafficking phenotype (Fig. 2). As measured by HA-antibody binding of external HA-epitope tagged channels (Fig.2A), the Δ314-15 mutation reduced cell surface expression to background levels, comparable to the effects of removing the “ER export” signal (ΔFCYE) (Ma et al., 2001). Confocal microscopy (Fig.2B) revealed that Kir2.1Δ314-15 channels co-localize with markers of the medial Golgi (GM130, (Nakamura et al., 1995)) and trans Golgi network (TGN46 or TGN38 (Prescott et al., 1997)), unlike the robust surface localization of the wild-type channel and the ER retention phenotype of

ΔFCYE-mutant channels. As evaluated by Person's co-localization analysis, the degree of Kir2.1Δ314-15 channel localization in the Golgi is significant.

Because the effects of ATS1 are notably manifested in the heart, we examined whether the unusual Golgi mistrafficking phenotype of the Δ314-15 mutant is recapitulated in cardiomyocytes. The issue is particularly germane because the Golgi exhibits an atypical subcellular distribution in cardiomyocytes, localizing throughout the cytoplasm within linear tracks between contractile bundles, similar to what has been described in skeletal muscle (Rahkila et al., 1997; Ralston, 1993). For these studies, wild-type and Δ314-15 Kir2.1 were delivered to adult rat ventricular myocytes by adenoviral-mediated cDNA transfer, and their subcellular localization was inspected by confocal microscopy (Fig. 2E–H). Wild-type channels localized to the cell surface and along tubular invaginations, characteristic of sarcolemmal and transverse-tubular localization of the endogenous channel (Melnyk et al., 2002). Kir2.1 Δ314-15 channels, by contrast, were entirely intracellular, accumulating in large puncta that co-localize with either GM130 (Fig. 2F) or TGN38 (Fig. 2G) in the Golgi. In fact, nearly all Kir2.1 Δ314-15 is contained within GM130 or TGN38 structures (Fig.2H). The steady-state co-localization of the mutant channel with trans- and cis-Golgi markers indicate the mutation blocks channel trafficking between the terminal Golgi cisterna and trans-Golgi network. In face of an uninterrupted and dominant ER-export process (Ma et al., 2001; Ma et al., 2002; Zerangue et al., 2001), mutant channels have no place to go except to amass within cis- and trans-Golgi compartments, causing Golgi structures to increase in size.

The Δ314-15 Mutation Blocks Golgi Export

Because the mutant channels are rapidly translocated from the Golgi into the endoplasmic reticulum upon Brefeldin A treatment, we suspected that Kir2.1Δ314-15 channels are retained in the Golgi by virtue of a block in signal-dependent anterograde trafficking rather than formation of insoluble aggregates (Kopito, 2000). To test this, we monitored Kir2.1 trafficking in the secretory pathway by several independent measures (Fig.3). Biosynthetic trafficking of Kir2.1 to the plasmalemma was studied by pulse-chase, cell surface immunoprecipitation (Fig.3A and B). In these studies, external HA-tagged channels were metabolically labeled in COS7 cells with a short pulse of S35-methionine (10 min) and then chased for variable times. Newly synthesized channels were captured at the plasmalemma by HA-immunoprecipitation and detected by autoradiography. As shown in Figure 3A–B, wild-type channels appeared at the plasmalemma within the first 10 minutes of the chase period and gradually increased thereafter. By contrast, Kir2.1Δ314-15 channels were not detected at the cell surface over the entire chase period. Thus, 314-15-dependent trafficking occurs early in the biosynthetic pathway, consistent with a Golgi exit mechanism.

To determine whether the trafficking step is harbored in the Golgi, Kir2.1 movement was monitored by live cell imaging (Fig.3C–D), using the reversible photoactivable fluorescent protein, Dronpa (Ando et al., 2004; Habuchi et al., 2005). For these studies, Dronpa-Kir2.1 fluorescence throughout the cell was first erased to background levels, and the population of channels at the Golgi (as detected with DS-red-Golgi) was specifically photoactivated and chased. Over time, the Golgi-delimited population of WT Dronpa-Kir 2.1, gradually diminished at a rate and kinetic comparable to the biosynthetic surface delivery (Fig.3C). These channels did not appear to accumulate in endosomes before they reached the cell surface, suggesting a direct trafficking route from the Golgi to the plasmalemma. By contrast, the Dronpa-Kir2.1Δ314–15 channel remained in the Golgi over the entire chase period. Taken together, the data indicate the trafficking operation is controlled at the Golgi (Fig.3C and D). Studies of glycosylation-state maturation revealed that the Δ314–15 mutation arrests traffic between the terminal cisterna and TGN, corroborating and extending these conclusions (Fig. S2).

Sequence Determinants of the Golgi Export Signal

The finding that the C-terminal ATS1 mutation blocks Golgi exit, identical to mutations in the N-terminal Golgi trafficking structure, suggests that the export signal is formed by neighboring residues in the tertiary structure. Trans-reconstitution studies offer further support for shared requirements of the juxtaposing N- and C- terminal structures; we found Golgi-export of N-terminal trunated channels can be restored upon co-expression of a polypetide encoding the Kir2.1 N-terminus unless the fragments harbor the ATS1 mutation or mutations in the key N-terminal residues (Fig. S3). To more precisely define the Golgi export structure, residues bordering the subunit interface were identified in the crystal structure and subjected to alanine replacement mutagenesis (Figure 4). External HA-tagged channels, bearing the mutations, were expressed in COS7 cells and the extent of traffic to the plasmalemma was quantified by cell surface antibody binding, and Golgi targeting was quantified by GM-130 co-localization (Fig.4A). Of the eighteen mutations tested, six shifted the localization of the channel from the cell surface to the Golgi, revealing necessary components of the Golgi trafficking structure. Of the N-terminal residues, R_{46} had the largest contribution but R_{44} exhibited additive effects. A tract of responsive mutations in the cytoplasmic C-terminus identified residues Y_{315}, E_{319}, I_{320}, and W_{322} as Golgi export determinants.

Mapping the residues in the crystal structure reveals a signal patch comprised of a composite of residues from separate cytoplasmic domains (Fig.4B). The side chains of all involved residues, except Y_{315}, project toward the solvent exposed surface, and, thus, are capable of acting collectively as a trafficking signal. Characterized in this way, the Golgi export signal, minimally involves a charged group of residues (R_{44}, R_{46}, E_{319}) at the N-terminal pole and a shallow, hydrophobic cleft ($I_{320}XW_{322}$) at the C-terminal pole. While it is conceivable that some of these residues indirectly participate in Golgi-export by holding the domains in close proximity or by participating in an allosteric transduction process, they collectively influence trafficking rather than govern domain association (Figure S4).

The Kir2.1 Golgi Export Structure is Transplantable

A hallmark of conventional trafficking signals is their ability to function as autonomous units. To explore this issue, we tested whether transplanting the Kir2.1 cytoplasmic domains onto the Human T lymphocyte membrane protein, CD8 (Littman et al., 1985) is sufficient to direct Golgi export (Fig. 5). The dimeric nature of CD8 makes it an ideal reporter for these studies (Jackson et al., 1993). Attachment of either the N- or the C-terminal domain alone onto the cytoplasmic side of CD8 rendered the reporter unable to reach the cell surface from the Golgi, confirming and extending our observations that neither domain alone is sufficient for Golgi export. To test if the Golgi export function requires the assembled cytoplasmic structure, we took advantage of the fact that the cytoplasmic N-and C-termini can be artificially joined together to form a properly folded cytoplasmic domain (Nishida and MacKinnon, 2002; Pegan et al., 2005). In contrast to CD8 reporters containing the isolated domains, robust surface expression was observed when CD8 was fused to the entire cytoplasmic domain (N+C) or when CD8-Kir2.1-N and the CD8-Kir2.1-C were co-expressed together. As predicted if the CD8 reporters recapitulate the Golgi trafficking signal of the native channel, the ATS1 Δ314–15 mutation blocked Golgi export. Thus, the Golgi export function is transplantable but uniquely requires both N- and C-cytoplasmic domains, consistent with an export signal within the tertiary structure.

Signal-Dependent Interaction with AP1 Clathrin Adaptor Complex drives Golgi Export

If the structure acts as a Golgi export signal, it should serve as a recognition site for Golgi trafficking machinery interaction. To explore this, a bacterial glutathione-Stransferase (GST) fusion protein of the entire Kir 2.1 cytoplasmic domain was used as a probe to test for its

interaction with the AP1 clathrin-adaptor and GGA1, molecules best known to facilitate export of cargo from the trans Golgi network (Bonifacino and Traub, 2003). This approach, using the entire cytoplasmic domain as an affinity ligand, allows the identification of proteins that bind to sites within the fully assembled cytoplasmic structure.

For initial studies, the WT GST-Kir 2.1 cytoplasmic domain (CD) was compared to mutant GST-Kir2.1 CD, harboring Δ314–315. Both fusion proteins are soluble and readily isolated to homogeneity under non-denaturing conditions (Fig.6A). The GST proteins were immobilized on glutathione-beads, incubated with a cytoplasmic extract that was enriched with AP1 and GGA, washed extensively and bound material was subjected to Western blot analysis with antibodies to AP1γ-adaptin subunit or GGA1. As controls, interaction of known Kir2.1 binding partners was examined. The Lin-7/CASK PDZ protein complex (Leonoudakis et al., 2004a; Leonoudakis et al., 2004b) and Filamin A (Sampson et al., 2003) bind to distinct sites on Kir2.1, separate from the Golgi export structure, and were therefore probed. As shown in Fig. 6B, the GST fusion of the WT-Kir2.1 cytoplasmic domain interacts with AP1 but not GGA1. Significantly, the Δ314–15 mutation abrogated AP1 binding without altering interaction with Lin-7, CASK or Filamin A, indicative of a specific disruption of a local AP1 binding site. As predicted for recognition of the Golgi trafficking signal, mutations in the Kir 2.1 residues that are required for Golgi export also completely abrogated AP1 binding (fig. 6C). Studies with recombinant AP1 subunits, prepared as hemicomplex forms (β1μ1 or γσ1) in insect cells (Doray et al., 2007), revealed the complementary interaction site is contained within the AP1 γσ1 subunits (fig. 6D).

To corroborate the interaction occurs within cells and is commensurate with Golgi export, co-immunoprecipitation (Fig.6E) and co-localization (Fig.6F) studies were performed in cells after trafficking at the trans-Golgi was released (37°C) from temperature-sensitive blockade (19°C) (Griffiths *et al.*1985; Saraste & Kuismanen, 1984). As predicted for a signal recognition event at the TGN, WT Kir2.1 channels co-localize and interact with AP1, but only after they are released from the temperature block and become competent to exit the Golgi. Moreover, the ATS1 mutation completely blocked the interaction, substantiating the in vitro binding studies.

To test whether AP1 facilitates the export of Kir2.1 from the Golgi, we examined Kir2.1 trafficking following siRNA mediated knockdown of the AP1 γ-adaptin subunit. As shown in Fig. 7, three different γ-adaptin siRNA probes had similar, specific effects, reducing AP1-γ-adaptin protein abundance without suppressing other proteins, such as β-actin (Fig.7A), or altering general Golgi structure (see characteristic localization of TGN46, Fig.7C). Ablation of AP1-γ-adaptin expression was paralleled by a significant reduction of Kir 2.1 at the cell surface (Fig.7B). As evidenced by the co-localization with TGN46, AP1-γ-adaptin knockout led to accumulation of the WT channel at the TGN (Fig. 7C), identical to the Golgi-mistrafficking phenotype of channels lacking the Golgi-export signal. A nearly identical inhibitory response was observed with the CD8-Kir2.1(NC) chimera, demonstrating the Golgi export signal is interpreted in AP1 dependent manner, even when transplanted. By contrast, AP1 depletion had no effect on the surface expression of influenza hemagglutinin (HA), a raft-associated transmembrane protein that leaves the TGN via a different mechanism. Expression of a siRNA-resistant form of gamma-adaptin rescued surface expression of WT Kir2.1 and the CD8-Kir2.1CD chimera, further documenting specificity. Taken together, the data reveals Kir2.1 channels are selected for export from the Golgi in a signal-dependent manner through an AP1 clathrin adaptor interaction.

DISCUSSION

Our data reveal a mechanism for sorting Kir2.1 channels at the Golgi for delivery to the cell surface, and provide insights into how newly synthesized plasmalemma-bound proteins can be exported from the Golgi in a signal dependent manner and disrupted in disease.

Golgi Export Patch as a Conformational Structure

The unique topological organization of the Golgi export patch provides a means to couple channel trafficking to protein conformation, similar to the ways that “conformational epitopes” specify sorting operations in Sec22 (Mancias and Goldberg, 2007) and other SNARE proteins (Miller et al., 2007; Pryor et al., 2008). Indeed, vesicle-sorting signals in SNAREs are located in surface patch structures, and dependent on overall folding. In Sec22, a COPII recognition signal is exposed in the unassembled state, allowing this SNARE to traffic from the ER to the Golgi in a non-fusogenic conformation (Mancias and Goldberg, 2007). Similarly, folding-dependent conformation of epsin and Hrb recognition sites in SNARE vti1b and VAMP7 provide a mechanism to coordinate post-fusion retrieval of SNARES into clathrin-coated endocytotic vesicles (Miller et al., 2007; Pryor et al., 2008). Recent crystallographic analysis of related bacterial Kir channels (Clarke et al., 2010) strongly suggest that the Golgi export patch in Kir2.1 is apart of a conformational structure, akin to the sorting signals found in SNAREs. Acquisition of the active potassium conduction state in these channels involves a rotation of the cytoplasmic domains and a reorientation of N- and C- termini. In Kir 2.1, the conformational change would allow residues from the two poles of the Golgi export patch, R_{46}- E_{319}, to form a salt bridge, and effectively juxtapose elements on both sides of the trafficking signal. Formation of the signal in this way would ensure only appropriately folded channels exit the Golgi, and offer an additional checkpoint for newly synthesized proteins beyond the well-known quality control processes in the endoplasmic reticulum (Ellgaard and Helenius, 2003). It also provides regulatory modality not found in conventional, linear trafficking signals. In fact, observations with the closely related Kir1.1 (ROMK) channel suggest that formation of the signal may be physiologically regulated to control surface delivery from the Golgi; this channel shares a similar sequence with the Golgi export patch in Kir2.1 but requires phosphorylation of a nearby residue to specify anterograde trafficking from the Golgi (O'Connell et al., 2005; Yoo et al., 2005; Yoo et al., 2003).

The Golgi Export Patch is an AP1 clathrin-adaptor recognition site

Although the signal patch identified in the present study is mechanistically different from conventional AP1 dependent Golgi-export signals, it drives transport from the Golgi by a related process. Comprised of four subunits, the AP-1 complex contains separate binding sites for clathrin and the canonical motif-containing trafficking signals. Clathrin interacts with the larger β1 subunit while tyrosine-based “YXXϕ” signals bind to the medium subunit, μ1(Ohno et al., 1995) and di-leucine signals ([DE]XXXL[LI]) (Bonifacino and Traub, 2003) interact with the γ/σ1 hemicomplex (Chaudhuri et al., 2007; Janvier et al., 2003). Similarly, because the γ/σ1 subunits harbor the recognition site for the Golgi-export signal in Kir2.1, far removed from the clathrin binding site in the β subunit hinge region (Shih et al., 1995), AP1 has the capacity to simultaneously engage clathrin and Kir2.1, and thereby select channels for inclusion into clathrin-coated Golgi-export carriers at the TGN. Because the Golgi export patch shares no resemblance to the canonical sorting motifs, the recognition mechanism is presumably much different. As a consequence, interaction of Kir2.1 with AP-1 will not complete with the binding of conventional motif-containing proteins, and allow concurrent binding. Such a mechanism may provide an additional mode to control the Golgi localization of AP1 together with the coincident binding of Arf-1, conventional sorting signals, and phosphoinositides (Lee et al., 2008).

Our observations expand the function of AP1 adaptin complex beyond its well-accepted endosomal-lysosomal cargo sorting activity (Bonifacino and Traub, 2003). They point to a more general function of AP1, whereby it selects different proteins as cargo for export from TGN, regardless of their final subcellular destinations. In principle, plasmalemma-bound proteins may be sorted by AP1 at the Golgi for itinerate trafficking through endosomes, but, within the resolution of our measurements, Kir2.1 channels travel rapidly, if not directly, to the cell surface from the Golgi. Future studies will be required to determine if AP1 can be modified to target proteins, like Kir 2.1, to the plasmalemma rather than the endosome. Clathrin adaptor function can be influenced by different accessory proteins (Baust et al., 2006; Crump et al., 2001; Lui et al., 2003), and certain GGAs (Doray et al., 2002). Perhaps, one or more of these operate with the AP1 complex to drive Golgi-to-surface trafficking of specific proteins, such as Kir2.1.

Physiological and Pathophysiological Implications

This study reveals a previously unappreciated locus of disease susceptibility. Of the 39 different ATS1 mutations that have been identified in the KCNJ2 gene, the majority disrupt PIP2-dependent Kir2.1 channel opening (Lopes et al., 2002; Ma et al., 2007), underscoring the importance of regulated Kir2.1 channel gating in myocyte excitability. Our study uncovered a critical regulatory step for controlling cell surface expression of the channel from the Golgi. The signal-dependent process provides a mechanism to control targeting of Kir2.1 to the sarcolemma and the transverse tubule at optimal densities for appropriate electrical signal transmission. Indeed, as exemplified by the uncoordinated excitation-contraction coupling, periodic paralysis and arrhythmias in ATS1(Tristani-Firouzi et al., 2002), a devastating state of muscle hyperexcitability develops when disruption of Golgi export process prevents Kir2.1 delivery to these specialized surface membranes. It will be important to learn if alterations in the Golgi export process can also account for other disorders that may arise from Kir2.1 mistrafficking, such as the proarrhythmic state of heart failure (Pogwizd and Bers, 2004). 40% of patients with Andersen-Tawil syndrome have no mutations in Kir2.1, and the genetic basis of the disease in these cases is completely unknown (Donaldson et al., 2004). In light of our findings, Golgi-export genes should be considered as candidates.

In summary, our observations provide insights into the mechanisms responsible for sorting plasmalemma-destined cargo at the Golgi. We propose that the location of the export signal within the confluence of the cytoplasmic domains provides a means to couple Golgi exit to protein conformation for quality control and regulation of cell surface density.

EXPERIMENTAL PROCEDURES

Antibodies and Plasmids

Details on antibodies and cDNA constructs used in this study are available as Extended Experimental Procedures, Table S1 and Table S2.

Cell Culture

COS7 cells and primary rat adult ventricular heart cells were cultured in high glucose DMEM (Invitrogene) containing 10% FBS, 100 U/ml penicillin/streptomycin (37°C, 5% CO_2).

Production and Infection of HA-tagged Kir2.1 Adenoviruses

Adenoviral vectors containing Kir2.1 channels were produced using AdEasy Adenoviral Vector System (Stratagene, Inc). Viruses were propagated in HEK293 cells and isolated as

before (Liu et al., 2001). Infection of rat adult heart cells was performed as previously described (Kohout et al., 1996).

RNA Interference

Three different double-stranded siRNA probes (Dharmacon, Inc) corresponding to nucleotides 528–548, 849–867, and 1102–1120 of the human AP1γ-adaptin subunit mRNA were used. COS-7 cells were transfected with either a non-silencing negative control siRNA duplex (Qiagen) or γ-adaptin siRNA targeted (20nM) using X-tremeGene (Roche Diagnostics). After 24hrs, the cells were transfected again with Kir2.1, CD8-Kir2.1 (N+C) or pCB6-HA (gift of Dr. Ora Weisz). After 36–48hrs, cells were processed for study. Four silent mutations were incorporated to generate a RNAi-resistant γ-adaptin probe.

Immunofluorescence and Confocal Microscopy

Cells were fixed (4% paraformaldehyde), permeabilized (0.1% Triton X-100), blocked (PBS + 5% FBS), incubated with primary antibody, washed in PBS and incubated with Alexa labeled secondary antibody. For some studies, channel proteins at the cell surface were first labeled with mouse anti-HA. Intracellular channel proteins were subsequently labeled with rabbit anti-HA after permeabilization. Goat anti-rabbit-Alexa-568 and goat anti-mouse-Alexa-488 were used as secondary antibodies to label intracellular and surface expressed channels. Cells were visualized by confocal laser-scanning microscopy (Zeiss-410 or Zeiss-510 meta) using a 63× oil immersion lens (NA1.40).

Quantitative Imaging analysis—Colocalization of channels and Golgi markers were quantified using a statistical algorithm (Costes et al., 2004) for calculation of Pearson's correlation and co-compartmentalization levels (Manders et al., 1992). The degree of channel compartmentalization in cardiomyocytes was calculated as the proportion of channel colocalized with the relevant markers (Manders et al., 1993). All procedures were performed with Volocity 4.2 (Improvision, UK).

Live cell imaging—COS7 cells were co-transfected with Dronpa-tagged Kir2.1 cDNA and pDsRed-Monomer-Golgi (Clontech). Cells were examined with 100× oil plan-Neofluar objective (NA 1.3) on a laser scanning confocal microscope (LSM 510, Zeiss) and studied at 37°C. Dronpa (Ando et al., 2004; Habuchi et al., 2005) was imaged and bleached using a 488 argon laser. Dronpa emission was isolated with a 505–550 bandpass filter. A 361nm Coherent Enterprise laser was used to reactivate Dronpa.

Quantitative Chemiluminescence Detection of Surface Proteins—To quantify Kir2.1 cell surface expression, COS7 cells were studied 36hrs after transfection, fixed (2% paraformaldehyde,10 minutes), blocked on ice (5% Fetal Bovine Serum in 1×PBS, 30min), incubated with mouse monoclonal anti-HA, or anti-CD8 (1:400, 1hour), washed (PBS, 3×, 5minutes), incubated with goat anti-mouse IgG HRP-conjugated secondary antibody (1:500), and then extensively washed (PBS, 5 minutes × 4). Cells were suspended in PBS, and aliquots were combined with SuperSignal ELISA Pico solution (Pierce Biotechnology). Chemiluminescence was measured in Relative Light Units (RLU) using an analytical luminometer (Ma et al., 2007) and normalized to Kir2.1 protein abundance. Reported values are the average of triplicate transfections from three different experiments.

GST fusion pull-down analysis—GST fusion proteins were purified under nondenaturing conditions on glutathione-agarose beads and prepared using standard methods outlined in Extended Experimental Procedures Table 3. GST fusion proteins were immobilized on glutathione beads and incubated with of rat brain lysates or recombinant AP-1 subunits. Rat brain lysates were prepared according to published protocols for AP-1

binding studies (Le Borgne et al., 1996). Recombinant AP1 subunits were expressed as epitope-tagged hemi-complexes (γ/σ1or β1/μ1 subunits, γ and β1 contained C-terminal epitopes for hemagglutinin (HA) and FLAG antibodies, respectively) from a bi-cistronic vector (pFast bac Dual, Invitrogen, AP-1 constructs gift of S. Kornberg) in Sf9 cells using baculovirus and then used for binding studies as previously described (Doray *et al*., 2007). Bound Proteins were detected in Western Blots with antibodies to AP1 clathrin adaptor, other interacting proteins or epitope tags. Immunoreactive bands were quantified by densitometry (NIH image, version 1.63f).

AP1-Kir2.1 immunoprecipitation—A procedure designed to capture transient AP1-cargo interactions, using the crosslinking reagent, DTSSP (Orzech *et al*., 1999) was used. Cells were permeabilized with digitonin (50ug/ml), washed, then incubated with the crosslinker (Themo Scientific) for 2hrs at 4°C. Crosslinker activity was quenched by incubation with 150mM glycine, pH 7.4, for 20 min at 22°C. Cell extracts were prepared, and Kir2.1-HA was subjected to immunoprecipitation with HA antibodies. Interaction AP1 was detected by Western analysis using antibodies to γ-adaptin. Interaction was accessed in cells that were incubated at 19°C (2 hrs) to block anterograde traffic of membrane proteins from TGN and after release from Golgi block (30 min, 37°C).

Kir2.1 channel surface delivery—COS7 cell suspensions were treated with a methinone and cysteine free medium (30 minutes, DMEM minus methionine and cysteine + 5% FBS), washed (1×PBS), and pulse-labeled with 100μCi/ml of ^{35}S-labelled Cys-Met mixture (MP Biomedicals Inc., Solon, OH) for 10 minutes at 37°C. Cells were, then, washed extensively (DMEM + 10mg/ml L-Met/Cys, 10%FBS) and chased at 37°C. Chase was stopped by rapid chilling, and cells were subjected to surface HA-immunoprecipitation for phosphoimaging analysis (Le Maout et al., 1997).

Statistical Analysis

Two-tail Student T-test and one-way ANOVA with Bonferroni's multiple comparison test were performed with Prism 4. $P<0.05$ was considered significant.

Supplementary Material

Refer to Web version on PubMed Central for supplementary material.

Acknowledgments

This project was supported by funds from the NIH (P01 HL70709, R01 DK54231, R01 DK 63049, T32-HL-072751) and the American Heart Association (0855321E). We thank Drs. Ora Weisz and S. Kornberg for reagents, Dr. Terry Rogers for support and advice, and Dr. William R. Randall for help with adenovirus production.

Literature Cited

Andersen ED, Krasilnikoff PA, Overvad H. Intermittent muscular weakness, extrasystoles, and multiple developmental anomalies. A new syndrome? Acta Paediatr Scand. 1971; 60:559–564. [PubMed: 4106724]

Ando R, Mizuno H, Miyawaki A. Regulated fast nucleocytoplasmic shuttling observed by reversible protein highlighting. Science. 2004; 306:1370–1373. [PubMed: 15550670]

Baust T, Czupalla C, Krause E, Bourel-Bonnet L, Hoflack B. Proteomic analysis of adaptor protein 1A coats selectively assembled on liposomes. Proc Natl Acad Sci U S A. 2006; 103:3159–3164. [PubMed: 16492770]

Bendahhou S, Donaldson MR, Plaster NM, Tristani-Firouzi M, Fu YH, Ptacek LJ. Defective potassium channel Kir2.1 trafficking underlies Andersen-Tawil syndrome. J Biol Chem. 2003; 278:51779–51785. [PubMed: 14522976]

Bonifacino JS, Traub LM. Signals for sorting of transmembrane proteins to endosomes and lysosomes. Annu Rev Biochem. 2003; 72:395–447. [PubMed: 12651740]

Campo C, Mason A, Maouyo D, Olsen O, Yoo D, Welling PA. Molecular mechanisms of membrane polarity in renal epithelial cells. Rev Physiol Biochem Pharmacol. 2005; 153:47–99. [PubMed: 15674648]

Chaudhuri R, Lindwasser OW, Smith WJ, Hurley JH, Bonifacino JS. CD4 Downregulation by HIV-1 Nef is Dependent on Clathrin and Involves a Direct Interaction of Nef with the AP2 Clathrin Adaptor. J Virol. 2007

Clarke OB, Caputo AT, Hill AP, Vandenberg JI, Smith BJ, Gulbis JM. Domain reorientation and rotation of an intracellular assembly regulate conduction in Kir potassium channels. Cell. 2010; 141:1018–1029. [PubMed: 20564790]

Costes SV, Daelemans D, Cho EH, Dobbin Z, Pavlakis G, Lockett S. Automatic and quantitative measurement of protein-protein colocalization in live cells. Biophys J. 2004; 86:3993–4003. [PubMed: 15189895]

Crump CM, Xiang Y, Thomas L, Gu F, Austin C, Tooze SA, Thomas G. PACS-1 binding to adaptors is required for acidic cluster motif-mediated protein traffic. EMBO Journal. 2001; 20:2191–2201. [PubMed: 11331585]

Deborde S, Perret E, Gravotta D, Deora A, Salvarezza S, Schreiner R, Rodriguez-Boulan E. Clathrin is a key regulator of basolateral polarity. Nature. 2008; 452:719–723. [PubMed: 18401403]

Donaldson MR, Yoon G, Fu YH, Ptacek LJ. Andersen-Tawil syndrome: a model of clinical variability, pleiotropy, and genetic heterogeneity. Ann Med. 2004; 36(Suppl 1):92–97. [PubMed: 15176430]

Doray B, Ghosh P, Griffith J, Geuze HJ, Kornfeld S. Cooperation of GGAs and AP-1 in packaging MPRs at the trans-Golgi network. Science. 2002; 297:1700–1703. [PubMed: 12215646]

Doray B, Lee I, Knisely J, Bu G, Kornfeld S. The gamma/sigma1 and alpha/sigma2 hemicomplexes of clathrin adaptors AP-1 and AP-2 harbor the dileucine recognition site. Mol Biol Cell. 2007; 18:1887–1896. [PubMed: 17360967]

Ellgaard L, Helenius A. Quality control in the endoplasmic reticulum. NatRevMolCell Biol. 2003; 4:181–191.

Fischer-Lougheed J, Liu JH, Espinos E, Mordasini D, Bader CR, Belin D, Bernheim L. Human myoblast fusion requires expression of functional inward rectifier Kir2.1 channels. J Cell Biol. 2001; 153:677–686. [PubMed: 11352930]

Godi A, Di Campli A, Konstantakopoulos A, Di Tullio G, Alessi DR, Kular GS, Daniele T, Marra P, Lucocq JM, De Matteis MA. FAPPs control Golgi-to-cell-surface membrane traffic by binding to ARF and PtdIns(4)P. Nat Cell Biol. 2004; 6:393–404. [PubMed: 15107860]

Habuchi S, Ando R, Dedecker P, Verheijen W, Mizuno H, Miyawaki A, Hofkens J. Reversible single-molecule photoswitching in the GFP-like fluorescent protein Dronpa. Proc Natl Acad Sci U S A. 2005; 102:9511–9516. [PubMed: 15972810]

Jackson MR, Nilsson T, Peterson PA. Retrieval of transmembrane proteins to the endoplasmic reticulum. J Cell Biol. 1993; 121:317–333. [PubMed: 8468349]

Janvier K, Kato Y, Boehm M, Rose JR, Martina JA, Kim BY, Venkatesan S, Bonifacino JS. Recognition of dileucine-based sorting signals from HIV-1 Nef and LIMP-II by the AP-1 gamma-sigma1 and AP-3 delta-sigma3 hemicomplexes. J Cell Biol. 2003; 163:1281–1290. [PubMed: 14691137]

Kohout TA, O'Brian JJ, Gaa ST, Lederer WJ, Rogers TB. Novel adenovirus component system that transfects cultured cardiac cells with high efficiency. Circ Res. 1996; 78:971–977. [PubMed: 8635247]

Kopito RR. Aggresomes, inclusion bodies and protein aggregation. Trends Cell Biol. 2000; 10:524–530. [PubMed: 11121744]

Kubo Y, Baldwin TJ, Jan YN, Jan LY. Primary structure and functional expression of a mouse inward rectifier potassium channel. Nature. 1993; 362:127–133. see comments. [PubMed: 7680768]

Le Borgne R, Griffiths G, Hoflack B. Mannose 6-phosphate receptors and ADP-ribosylation factors cooperate for high affinity interaction of the AP-1 Golgi assembly proteins with membranes. J Biol Chem. 1996; 271:2162–2170. [PubMed: 8567674]

Le Maout S, Brejon M, Olsen O, Merot J, Welling PA. Basolateral membrane targeting of a renal-epithelial inwardly rectifying potassium channel from the cortical collecting duct, CCD-IRK3, in MDCK cells. Proc Natl Acad Sci U S A. 1997; 94:13329–13334. [PubMed: 9371845]

Lee I, Doray B, Govero J, Kornfeld S. Binding of cargo sorting signals to AP-1 enhances its association with ADP ribosylation factor 1-GTP. J Cell Biol. 2008; 180:467–472. [PubMed: 18250197]

Leonoudakis D, Conti LR, Anderson S, Radeke CM, McGuire LM, Adams ME, Froehner SC, Yates JR, Vandenberg CA. Protein trafficking and anchoring complexes revealed by proteomic analysis of inward rectifier potassium channel (Kir2.x)-associated proteins. J Biol Chem. 2004a; 279:22331–22346. [PubMed: 15024025]

Leonoudakis D, Conti LR, Radeke CM, McGuire LM, Vandenberg CA. A multiprotein trafficking complex composed of SAP97, CASK, Veli, and Mint1 is associated with inward rectifier Kir2 potassium channels. J Biol Chem. 2004b; 279:19051–19063. [PubMed: 14960569]

Littman DR, Thomas Y, Maddon PJ, Chess L, Axel R. The isolation and sequence of the gene encoding T8: a molecule defining functional classes of T lymphocytes. Cell. 1985; 40:237–246. [PubMed: 3871356]

Liu Y, Cseresnyes Z, Randall WR, Schneider MF. Activity-dependent nuclear translocation and intranuclear distribution of NFATc in adult skeletal muscle fibers. J Cell Biol. 2001; 155:27–39. [PubMed: 11581284]

Lock JG, Hammond LA, Houghton F, Gleeson PA, Stow JL. E-cadherin transport from the trans-Golgi network in tubulovesicular carriers is selectively regulated by golgin-97. Traffic. 2005; 6:1142–1156. [PubMed: 16262725]

Lopes CM, Zhang H, Rohacs T, Jin T, Yang J, Logothetis DE. Alterations in conserved Kir channel-PIP2 interactions underlie channelopathies. Neuron. 2002; 34:933–944. [PubMed: 12086641]

Lui WW, Collins BM, Hirst J, Motley A, Millar C, Schu P, Owen DJ, Robinson MS. Binding partners for the COOH-terminal appendage domains of the GGAs and gamma-adaptin. Mol Biol Cell. 2003; 14:2385–2398. [PubMed: 12808037]

Ma D, Tang XD, Rogers TB, Welling PA. An andersen-Tawil syndrome mutation in Kir2.1 (V302M) alters the G-loop cytoplasmic K+ conduction pathway. J Biol Chem. 2007; 282:5781–5789. [PubMed: 17166852]

Ma D, Zerangue N, Lin YF, Collins A, Yu M, Jan YN, Jan LY. Role of ER export signals in controlling surface potassium channel numbers. Science. 2001; 291:316–339. [PubMed: 11209084]

Ma D, Zerangue N, Raab-Graham K, Fried SR, Jan YN, Jan LY. Diverse trafficking patterns due to multiple traffic motifs in G protein-activated inwardly rectifying potassium channels from brain and heart. Neuron. 2002; 33:715–729. [PubMed: 11879649]

Mancias JD, Goldberg J. The transport signal on Sec22 for packaging into COPII-coated vesicles is a conformational epitope. Mol Cell. 2007; 26:403–414. [PubMed: 17499046]

Manders EM, Stap J, Brakenhoff GJ, van Driel R, Aten JA. Dynamics of three-dimensional replication patterns during the S-phase, analysed by double labelling of DNA and confocal microscopy. J Cell Sci. 1992; 103(Pt 3):857–862. [PubMed: 1478975]

Manders EM, Verbeek FJ, Aten JA. Measurement of colocalization of objects in dual-color confocal images. Journal of Microscopy. 1993; 375:382.

Melnyk P, Zhang L, Shrier A, Nattel S. Differential distribution of Kir2.1 and Kir2.3 subunits in canine atrium and ventricle. Am J Physiol Heart Circ Physiol. 2002; 283:H1123–1133. [PubMed: 12181143]

Miller SE, Collins BM, McCoy AJ, Robinson MS, Owen DJ. A SNARE-adaptor interaction is a new mode of cargo recognition in clathrin-coated vesicles. Nature. 2007; 450:570–574. [PubMed: 18033301]

Nakamura N, Rabouille C, Watson R, Nilsson T, Hui N, Slusarewicz P, Kreis TE, Warren G. Characterization of a cis-Golgi matrix protein, GM130. J Cell Biol. 1995; 131:1715–1726. [PubMed: 8557739]

Nichols CG, Lopatin AN. Inward rectifier potassium channels. Annual Review of Physiology. 1997; 59:171–191. [Review] [177 refs].

Nishida M, MacKinnon R. Structural basis of inward rectification: cytoplasmic pore of the G protein-gated inward rectifier GIRK1 at 1.8 A resolution. Cell. 2002; 111:957–965. [PubMed: 12507423]

O'Connell AD, Leng Q, Dong K, MacGregor GG, Giebisch G, Hebert SC. Phosphorylation-regulated endoplasmic reticulum retention signal in the renal outer-medullary K+ channel (ROMK). Proc Natl Acad Sci U S A. 2005; 102:9954–9959. [PubMed: 15987778]

Ohno H, Stewart J, Fournier MC, Bosshart H, Rhee I, Miyatake S, Gallusser A, Kirchhausen T, Bonifacino JS. Interaction of tyrosine-based sorting signals with clathrin-associated proteins. Science. 1995; 269:1872–1875. [PubMed: 7569928]

Pegan S, Arrabit C, Zhou W, Kwiatkowski W, Collins A, Slesinger PA, Choe S. Cytoplasmic domain structures of Kir2.1 and Kir3.1 show sites for modulating gating and rectification. Nat Neurosci. 2005; 8:279–287. [PubMed: 15723059]

Plaster NM, Tawil R, Tristani-Firouzi M, Canun S, Bendahhou S, Tsunoda A, Donaldson MR, Iannaccone ST, Brunt E, Barohn R, et al. Mutations in Kir2.1 cause the developmental and episodic electrical phenotypes of Andersen's syndrome. Cell. 2001; 105:511–519. [PubMed: 11371347]

Pogwizd SM, Bers DM. Cellular basis of triggered arrhythmias in heart failure. Trends Cardiovasc Med. 2004; 14:61–66. [PubMed: 15030791]

Prescott AR, Lucocq JM, James J, Lister JM, Ponnambalam S. Distinct compartmentalization of TGN46 and beta 1,4-galactosyltransferase in HeLa cells. Eur J Cell Biol. 1997; 72:238–246. [PubMed: 9084986]

Pryor PR, Jackson L, Gray SR, Edeling MA, Thompson A, Sanderson CM, Evans PR, Owen DJ, Luzio JP. Molecular basis for the sorting of the SNARE VAMP7 into endocytic clathrin-coated vesicles by the ArfGAP Hrb. Cell. 2008; 134:817–827. [PubMed: 18775314]

Rahkila P, Vaananen K, Saraste J, Metsikko K. Endoplasmic reticulum to Golgi trafficking in multinucleated skeletal muscle fibers. Exp Cell Res. 1997; 234:452–464. [PubMed: 9260916]

Ralston E. Changes in architecture of the Golgi complex and other subcellular organelles during myogenesis. J Cell Biol. 1993; 120:399–409. [PubMed: 7678420]

Rodriguez-Boulan E, Musch A. Protein sorting in the Golgi complex: shifting paradigms. Biochim Biophys Acta. 2005; 1744:455–464. [PubMed: 15927284]

Sampson LJ, Leyland ML, Dart C. Direct interaction between the actin-binding protein filamin-A and the inwardly rectifying potassium channel, Kir2.1. J Biol Chem. 2003; 278:41988–41997. [PubMed: 12923176]

Sansone V, Griggs RC, Meola G, Ptacek LJ, Barohn R, Iannaccone S, Bryan W, Baker N, Janas SJ, Scott W, et al. Andersen's syndrome: a distinct periodic paralysis. Ann Neurol. 1997; 42:305–312. [PubMed: 9307251]

Shih W, Gallusser A, Kirchhausen T. A clathrin-binding site in the hinge of the beta 2 chain of mammalian AP-2 complexes. J Biol Chem. 1995; 270:31083–31090. [PubMed: 8537368]

Stockklausner C, Klocker N. Surface expression of inward rectifier potassium channels is controlled by selective Golgi export. J Biol Chem. 2003; 278:17000–17005. [PubMed: 12609985]

Tristani-Firouzi M, Jensen JL, Donaldson MR, Sansone V, Meola G, Hahn A, Bendahhou S, Kwiecinski H, Fidzianska A, Plaster N, et al. Functional and clinical characterization of KCNJ2 mutations associated with LQT7 (Andersen syndrome). J Clin Invest. 2002; 110:381–388. [PubMed: 12163457]

Wang CW, Hamamoto S, Orci L, Schekman R. Exomer: A coat complex for transport of select membrane proteins from the trans-Golgi network to the plasma membrane in yeast. J Cell Biol. 2006; 174:973–983. [PubMed: 17000877]

Yoo D, Fang L, Mason A, Kim BY, Welling PA. A phosphorylation-dependent export structure in ROMK (Kir 1.1) channel overrides an endoplasmic reticulum localization signal. J Biol Chem. 2005; 280:35281–35289. [PubMed: 16118216]

Yoo D, Kim BY, Campo C, Nance L, King A, Maouyo D, Welling PA. Cell surface expression of the ROMK (Kir 1.1) channel is regulated by the aldosterone-induced kinase, SGK-1, and protein kinase A. J Biol Chem. 2003; 278:23066–23075. [PubMed: 12684516]

Zaritsky JJ, Redell JB, Tempel BL, Schwarz TL. The consequences of disrupting cardiac inwardly rectifying K(+) current (I(K1)) as revealed by the targeted deletion of the murine Kir2.1 and Kir2.2 genes. J Physiol. 2001; 533:697–710. [PubMed: 11410627]

Zerangue N, Malan MJ, Fried SR, Dazin PF, Jan YN, Jan LY, Schwappach B. Analysis of endoplasmic reticulum trafficking signals by combinatorial screening in mammalian cells. ProcNatlAcadSciUSA. 2001; 98:2431–2436.

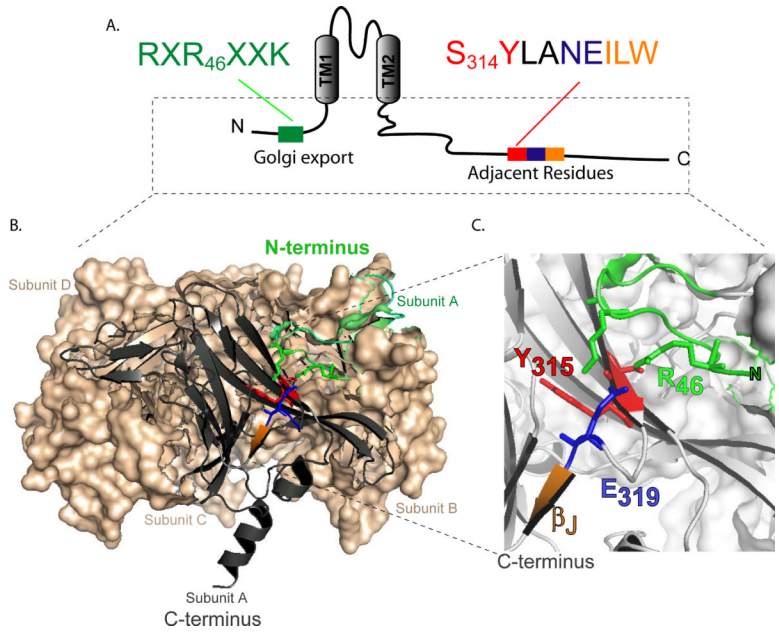

Figure 1. The Kir2.1 N-terminal Golgi export structure juxtaposes the cytoplasmic C-terminus and an ATS1 mutation

A. A single Kir2.1 channel subunit with relevant residues color-coded. (N-terminus, green; ATS1 mutation (Δ314-315), red; NE319, blue; hydrophobic residues in the Beta J stand, orange; transmembrane domains (TM1 and TM2), grey). **B**. Atomic structure Kir2.1 cytoplasmic domains channel tetramer, forming the cytoplasmic pore are shown (from Pegan et al. PDB1u4f). Standard ribbon display of one subunit (subunit A) is highlighted against a surface rendering of the other three subunits. **C**. Magnified view of residues at the cytoplasmic domain interface. Residues affected by the Δ314-15 ATS1 mutation, $SY_{314\text{-}15}$(red), lie under the N-terminal trafficking determinant (green).

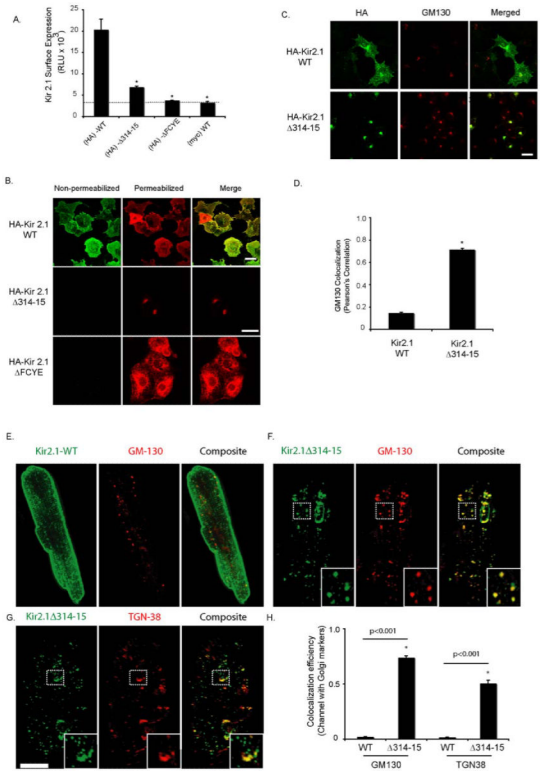

Figure 2. The Kir2.1 ATS1 mutant, Δ314-15, accumulates in the Golgi

A. Cell surface expression quantified by HA-antibody binding and luminometry in COS7 cells expressing external HA-tagged Kir2.1(wt), Kir2.1Δ314-15 or the ER-export defective mutant, Δ FCYENE. External myc-tagged Kir channels (myc-wt) were used as a negative control. (RLU, Relative Light Units.). **B**. Immunocytochemical analysis of external HA-tagged Kir2.1 channels in intact (red) and permeabilized (green) COS7 cells. **C**. Co-localization of Kir 2.1 Δ314-15 with the Golgi marker, GM130. **D**. Pearson's correlation of GM130 co-localization with HA-Kir2.1Δ314-315 (Mean ± S.E.M., n=49 cells from three transfections, * $P < 0.001$). **E-G**. Kir2.1Δ314-15 channels accumulate in Golgi structures of adult rat ventricular cardiomyocytes. Shown are 3-D rendered confocal serial sections of typical cardiomyocytes of either WT Kir2.1 or Kir2.1Δ314-15 with Golgi markers. Contrasting the localization of the WT Kir2.1 (E) at the t-tubule and sarcolemma, the mutant Δ314-15 channel co-localizes with (F) GM130 and (G) TGN-38 in the cis and trans-Golgi network (see magnified insets). H. Quantification of co-localization (mean ± S.E.M., n=20, *, $P < 0.001$). Scale bar =14 μm. (See also supplementary Fig.1).

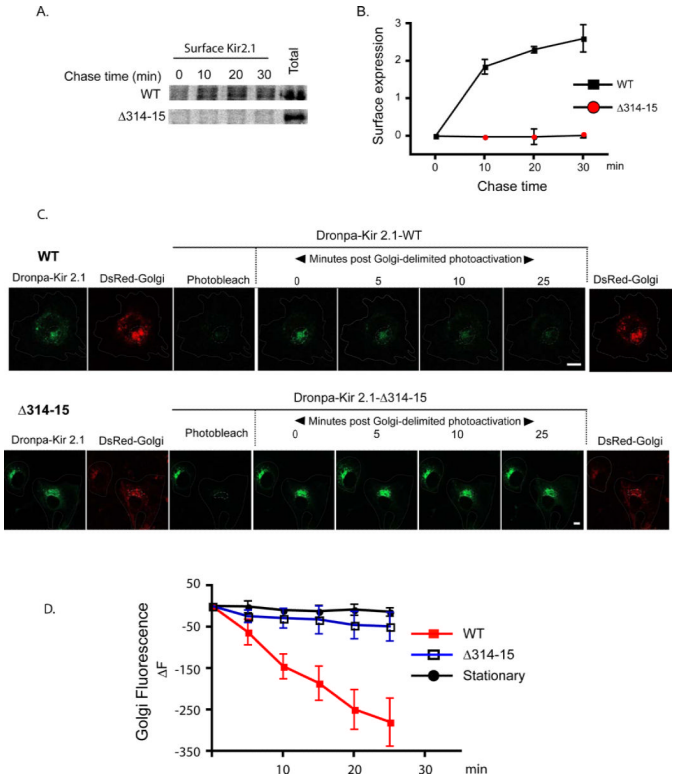

Figure 3. The Δ314-15 mutation blocks forward trafficking at the Golgi

A. Pulse-chase, cell-surface immunoprecipitation: Newly synthesized channels (external HA-tagged, Wild-type, WT and Δ314-15) were captured at the plasmalemma by surface HA-immunoprecipitation at the indicated chase times (10 minutes after metabolic labeling), detected by autoradiography and then compared to the total cellular signal. **B**. Quantification of the autoradiography (N= 3). **C**-**D**. Movement of Kir2.1 at the Golgi (WT and Δ314-315) was monitored in live COS7 cells using the reversible photoactivable protein, Dronpa. **C**. Shown are representative cells, studied when most of the WT Dropna-Kir2.1 channel is still located in the ER and Golgi. After total cellular fluorescence (outline traced in white) was bleached to background levels ("Photobleach"), Dronpa- was specifically photoactivated within the Golgi (dotted white line, as detected with DS-red-Golgi marker), and time-lapsed images were acquired ("Post photoactivation"). **D**. Quantification of the Dronpa fluorescent signal at the Golgi after photoactivation. Results are shown relative to a stationary marker (mean ± S.E.M., n=8). Bar =10 μm (See also supplementary Fig.2)

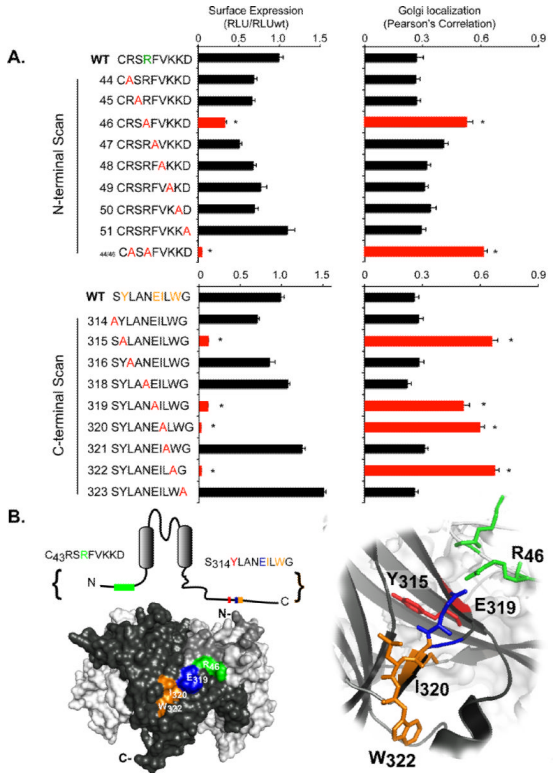

Figure 4. Golgi export signal sequence elucidated by structure-guided mutagenesis

A. Cell surface expression and Golgi localization of external HA-tagged Kir2.1 channels as quantified by surface HA-antibody binding (mean ± S.E.M., n=6, *p<0.001, cell surface normalized to total protein abundance) and co-localization with the Golgi marker GM130, using Person's correlation (mean ± S.E.M., n=15, *p<0.001). Results of alanine-substitution mutations in the cytoplasmic N- terminal region in the cytoplasmic C- terminus are shown in the top and bottom panels, respectfully. **B**. Key residues in the Kir2.1 cytoplasmic domain structure (PDB ID 1u4f). Left, surface rendering of the structure, showing residues in the Golgi export signal whose side chains project toward the solvent exposed surface. Residues are shown in one subunit (highlighted in dark) of a tetramer. Right, key residues are shown in a magnified view of the N-C interface. Relevant residues are color-coded. (See also supplementary Fig.3)

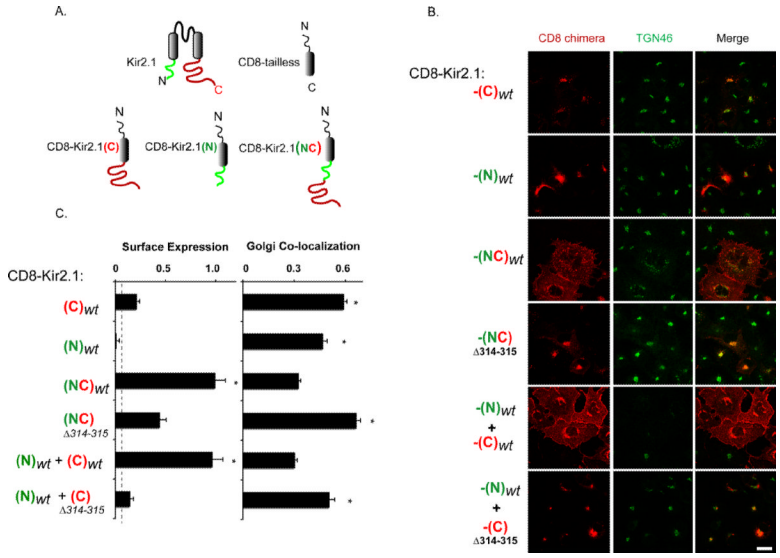

Figure 5. Transplantable Golgi export signal requires cytoplasmic N- and C- terminal domains

A. Cartoon of the CD8-Kir2.1 chimeras. CD8-Kir2.1(C) contains the extracellular and transmembrane domains of CD8 tailless fused to the Kir2.1 C-terminal domain. CD8-Kir2.1(N) is comprised of CD8 tailless fused to the Kir2.1 N-terminal domain. CD8-Kir2.1(NC) is a fusion of CD8 tailless with the entire Kir2.1 N-C cytoplasmic domain. Chimeras containing wild-type sequences are indicated "wt"; those bearing the ATS1 mutation are indicated as "Δ314-315". **B**. Immunolocalization of the indicated CD8 chimeras, detected with anti-CD8 antibodies (red) and the trans-Golgi marker, TGN46 (green). **C**. Cell surface expression was quantified by surface anti-CD8 binding and luminometry (mean ± S.E.M., n=8, *p<0.001, the cell surface normalized to total protein abundance of chimera). Golgi localization was quantified by Person's co-localization with TGN46. (mean ± S.E.M., n=20, *p<0.001) Scale bar = 25 μm

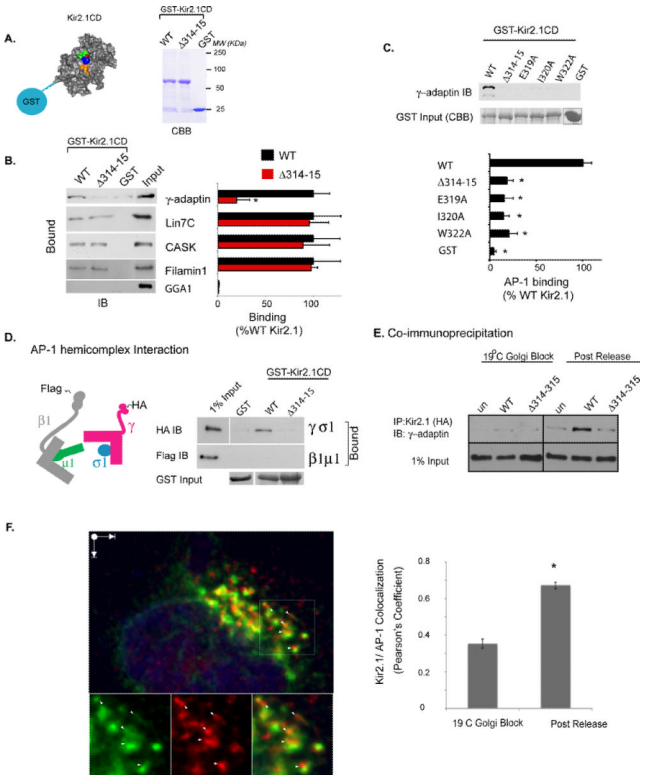

Figure 6. The AP1 clathrin adaptor interacts with the Kir2.1 Golgi export signal at the TGN

A. GST and GST-Kir2.1 fusion proteins (WT and the Δ314-15 mutant) following SDS-PAGE and Coomassie Brilliant Blue Staining (CBB). **B**. Proteins bound to the Kir2.1 cytoplasmic domain (CD) were detected by immunoblot (IB) with indicated antibodies and quantified by densitometry. The Δ314-15 mutation specifically reduced AP-1, γ binding without affecting interaction to the Lin-7/CASK complex and Filamin A (mean ± S.E.M., n=4, *p<0.01). **C**. Mutations in the Kir2.1 Golgi-export signal disrupt AP-1, γ interaction. AP-1, γ bound to each of the GST-Kir2.1 fusion proteins (CBB) was detected by immunoblot with γ specific antibodies and quantified (mean ± S.E.M., n=4, *p<0.01). **D**. The AP-1 interaction site for the Golgi export signal is harbored with in the γσ1 subunits. Recombinant AP1 subunits were prepared as the indicated hemicomplex forms in insect cells (β1μ-1 or γσ1, β1 and γ were tagged with the Flag or HA epitopes) and tested for direct interaction with GST alone or GST-Kir2.1CD (WT vs. Δ314-15). Bound AP1 subunit was detected in Western blots using anti-epitope tag antibodies. Shown is a representative experiment N=3 **E**. Immunoprecipitation (IP) of HA-tagged Kir2.1 (WT or Δ314-15 Kir2.1compared to untransfected controls) followed by immunoblotting (IB) with anti-AP1 γ antibodies in COS7 cells before and after trafficking at the trans-Golgi was released (37°C) from temperature-sensitive Golgi export blockade (19°C). **F**. Co-localization of EGFP-Kir2.1 with AP1 (Kir2.1, green; AP1γ, red; nucleus stained blue with DAP1). Upon release from block, Kir2.1 channels travel out of large cisternal structures, and then transiently co-localize with AP1 at the TGN before they exit in vesicles and tubules. Shown is a representative cell at 15 min into chase, when Kir2.1 is observed each of these structures. Arrowheads highlight several TGN structures, where Kir2.1 and AP1 co-localize, and where tubulo-vesicular carriers, containing the channel as cargo, are emerging. Boxed area, above, is shown below in individual color panels. Scale bar = 2.5 μm. **E**. Quantification of co-localization, before and after release from temperature block (mean ± S.E.M, N=8, * P < 0.001).

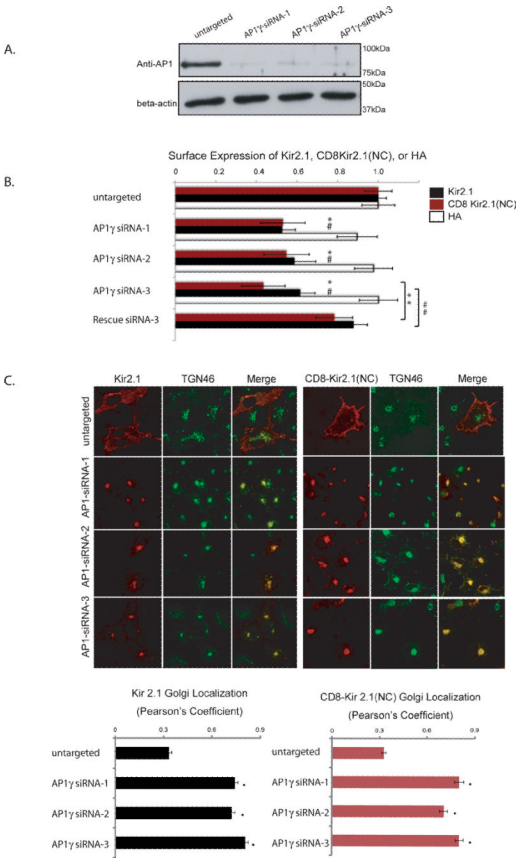

Figure 7. The AP1 clathrin adaptor targets the channel for Golgi export

A. Western blots of AP-1-γ-adaptin or actin in cells individually treated three different AP1γ siRNA probes (AP1 γ-siRNA1-3) or a negative control probe (siRNA-untargeted). **B**. As measured by surface antibody binding, AP-1-γ knockdown by each probe caused a significant reduction in Kir 2.1 (Black bars, *p<0.001, mean+S.E.M., n=5) or CD8-Kir2.1 (NC) (red bars, #p<0.001, n=5) but not influenza hemagglutinin (HA) (open bars, n=5) at the plasmalemma. Expression of RNAi resistant AP-1-γ (rescue) with the knockdown probe restored surface expression of Kir 2.1 and CD8-Kir2.1(NC) (##p<0.001, n= 5) **C**. Localization of HA-Kir2.1 (red, left pannels), or CD8-Kir2.1(NC) (red, right panels) and TGN46 (green), in cells transfected with the indicated RNAi probes. Golgi localization was quantified by Person's co-localization with TGN46. (mean ± S.E.M., n=10, *p<0.001)